Intrinsic stickiness in open integrable billiards: tiny border effects

M. S. Custódio and M. W. Beims[1, *]

[1] *Departamento de Física, Universidade Federal do Paraná, 81531-990 Curitiba, PR, Brazil*

(Dated: May 4, 2010)

Rounding border effects at the escape point of open integrable billiards are analyzed via the escape times statistics and emission angles. The model is the rectangular billiard and the shape of the escape point is assumed to have a semicircular form. Stickiness and self-similar structures for the escape times and emission angles are generated inside "backgammon" like stripes of initial conditions. These stripes are born at the boundary between two different emission angles but same escape times. As the rounding effects increase, backgammon stripes start to overlap and the escape times statistics obeys the power law decay and anomalous diffusion is expected. Tiny rounded borders (around 0.1% from the whole billiard size) are shown to be sufficient to generate the sticky motion, while borders larger than 10% are enough to produce escape times with chaotic decay.

PACS numbers: 05.45.-a,05.45.Ac
Keywords: Open billiards, self-similarity, rounded borders, stickiness.

I. INTRODUCTION

Experiments usually measure a signal (light, atoms, particles current etc) which comes out from the system of interest. If the open set (the escape point or hole) of the physical device, where the signal comes out, has a relevant size and shape, the signal may include informations from inside the physical device *and* from the open set itself. The shape and size of the open set depends on experimental interests but also on how the device is build. For the dynamics in mesoscopic systems and nanostructures, for example, the shape and the size of the small open set can present irregularities or defects which may induce undesirable changes in the outcoming signal. Such sometimes intrinsic irregularities affect the dynamics of particles which collide with them.

From the theoretical point of view it is very difficult to describe, in general, the dynamics of colliding particles with irregular boundaries. Therefore in recent years more and more attention has been given to the description of particles confined inside boundaries (or billiards) which present some *specific* edges, softness etc. To mention some examples we have the edge roughness in quantum dots [1], unusual boundary conditions in two-dimensional billiards [2, 3], effects of soft walls [4] and edge collisions [5] of interacting particles in a 1D billiard, rounding edge [6] and edge corrections [7] in a resonator, deformation of dielectric cavities [8], edge diffractions and the corresponding semiclassical quantization [9, 10], among others.

Different from the above works, which focus on the boundaries of systems, here we analyze the effect of irregularities from the open set itself. What is the effect of (rounded) open sets on the outcoming signal ? To mention some examples, rounded open sets are common in experiments with semiconductors devices [11, 12] and quantum cavities [13], where the open sets have a shape very similar to those shown in Fig. 1, which is the model used here (Type I and II). In the above mentioned experiments the ratio between the open set (not its width, but the radius of the rounded border) and the whole device lies around ~ 0.001 for Type II borders (the smallest case) and around ~ 0.3 for Type I borders (the largest case). Since experiments measure a signal which comes out from the system of interest, how is it affected by such rounded borders ? is it possible that tiny rounded borders transform an integrable dynamics into a chaotic one ? what is their influence on the dynamics in open nanodevices, conduction fluctuations in semiconductors [11, 14], particles transport in nanostructures, cold atoms in open optical billiards [15] etc? Recent works [16–19] in this direction analyzed the effect of the *width* of the open set on the escape rates of particles in open billiards.

Using the example of a billiard model we show here that the *shape* or *structure* of the open set induces stickiness [20], self-similar and a chaotic output signal, even if the dynamics inside the billiard is originally regular. We consider that the device borders (or extremities), which delimit the holes in realistic open systems, are not single points, but have their own shape. In this work results are shown for the escape times (ETs) statistics and the emission angles θ_f in the open rectangular billiard shown in Fig. 1. While self-similar structures are clearly visible in the ETs and escape angles, the sticky motion is observed by the power law decay of the ETs statistic. Although it is possible to detect and quantify sticky motion via the distribution of finite time Lyapunov exponents [4, 5, 21–23], for the purpose of the present work it is more adequate to use the ETs statistics. The fractal behavior of the ETs dynamics was also shown recently in Bose-Einstein condensates [24], trapped ultracold atoms [25] and in a vase-shaped cavity [26], in generic chaotic cavities [27], just to mention some examples.

The paper is organized as follows. Section II presents the model, defines the ETs used to detect the sticky behavior and shows related numerical results. Sections III

* E-mail address: mbeims@fisica.ufpr.br

and IV show the rich dynamics generated by the rounded border: long-lived states and self-similar structures for the ETs and emission angles. In Section V we present our final remarks.

II. ROUNDING BORDERS GENERATING STICKINESS

The ETs statistic is defined [28] by $Q(\tau) = \lim_{N\to\infty} \frac{N_\tau}{N}$, where N is the total number of trajectories which escape the billiard and N_τ is the number of trajectories which escape the billiard after the time τ. For systems with stickiness the ETs statistic decays as a power law [28] $Q(\tau) \propto \tau^{-\gamma_{esc}}$, where $\gamma_{esc} > 1$ is the scaling exponent. For hyperbolic chaotic systems and long times the ETs statistic decays exponentially. It is known that the diffusion exponent μ from the mean square displacement of the position $\langle x^2 \rangle \sim t^\mu$, is related to γ_{esc} via $\mu = 3 - \gamma_{esc}$ [29, 30].

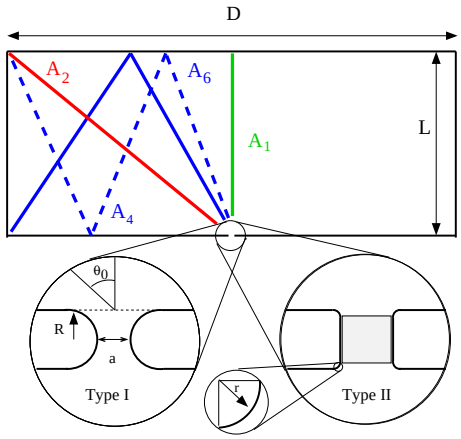

FIG. 1. (Color online) The rectangular billiard, with dimension $L \times D$, showing the open sets (borders) of Type I (with radius R) and Type II (radius $r \approx R/20$) considerer here. The escape point lies exactly in the middle of the billiard and has constant aperture $a = 1\times10^{-4}$. Initial angle θ_0 and, schematically, the shortest escape trajectories (A_1, A_2, A_4 and A_6) are shown. In all simulations we use $L = 4$ and $D = 10$.

In the simulations, particles start at times $t = 0$ from the escape point with an initial angle θ_0 towards the inner part of the billiard with velocity $|\vec{v}| = 1$. The particle suffers elastic collisions at the billiard boundaries and at the rounded border of the open set. For each initial condition we wait until the particle leaves the billiard and record θ_f and the ETs. We use 10^5 initial conditions distributed uniformly in the interval $0.10 \lesssim \theta_0 \lesssim 1.54$. The dynamics for $0.0 \leq \theta_0 \leq -\pi/2$ is symmetric. Without rounding effects ($R = r = 0$) the rectangular billiard is integrable and has zero Lyapunov exponents. As the ratio R/L increases, the rounded border acts like a dispersing boundary generating chaotic motion without regular islands. For larger values of R/L and some specific initial conditions, the dynamics should be equivalent to those obtained in the Sinai [31] and Bunimovich stadium [32] billiards. These billiard have marginally unstable periodic orbits (MUPOs), which are orbits bouncing perpendicularly between the parallel walls, and are known [19, 33] to generate the sticky exponent $\gamma_{esc} = 2$ for the ETs. In the rectangular billiard the MUPOs are obtained from the initial conditions $\theta = 0, \pi/2$. Therefore, in our case we also expect to see $\gamma_{esc} \to 2$ as R/L increases.

We start discussing numerically the quantity $Q(\tau)$ for the Type I billiard and for different values of the ratio R/L, where L is kept fixed. Results are shown in Fig. 2 for $R/L = 0, 1/10000, 1/1000, 1/100, 1/10$ and 1. Note that these results are automatically applied to the Type II billiard with $r/L \sim 0, 1/200000, 1/20000, 1/2000, 1/200$ and $1/20$, respectively. The only difference is that for the type II billiard the escape time τ' is related to τ by $\tau + t_p$, where t_p is the time the trajectory needs to travel the two parallel boundaries from the escape hole (see Type II border in Fig. 1). First observation is that for $R/L = 0$,

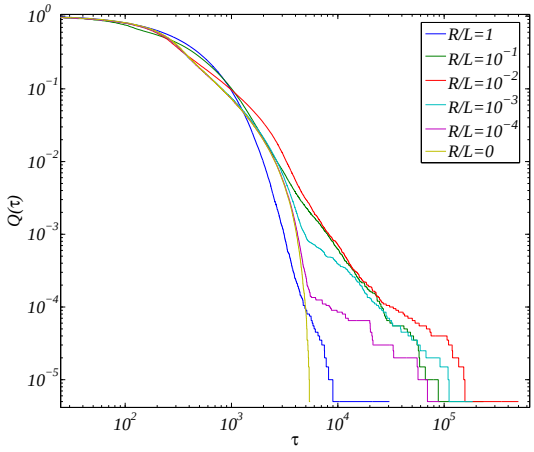

FIG. 2. (Color online) Behavior of $Q(\tau)$ for different values of the ratio R/L.

$Q(\tau)$ did not has a power law (neither an exponential decay). This is the integrable case and the maximal ET found is $\tau \sim 5.7 \times 10^2$. Such maximal time is obtained because we did not start initial conditions close to the MUPOs ($\theta = 0, \pi/2$). Separately (not shown) we used only initial conditions very close to the MUPOs. We found that $Q(\tau)$ did not have a finite maximal time, but a power law tail for very long times with $\gamma_{esc} \sim 1$. This shows that the MUPOs without the dispersing component (and no chaotic motion), does not generates the exponent $\gamma_{esc} \sim 2$. This agrees with results obtained [19] for some specific initial conditions in an open billiard.

For very small rounding effects, $R/L = 1/10000$, the qualitative behavior of $Q(\tau)$ starts to change (when compared to the case $R/L = 0$) for times $\tau \gtrsim 5.7 \times 10^2$, i. e. for those trajectories which stay longer inside the

billiard. This means that the very few trajectories which collide with the rounded border tend to stay longer inside the billiard and also change the qualitative behavior of $Q(\tau)$. The fitted escape exponent is $\gamma_{esc} \sim 0.6$. By increasing the border to $R/L = 1/1000$, we observe a power law decay in Fig. 2 for times $\tau \gtrsim 5.5 \times 10^2$. The escape exponent is $\gamma_{esc} \sim 1.3$. For $R/L = 1/100$ and $\tau \gtrsim 3\times10^3$ we obtain $\gamma_{esc} \sim 1.8$ and for $R/L = 1/10$ and $\tau \gtrsim 1\times10^3$ we obtain $\gamma_{esc} \sim 2.1$. From these points is it possible to get $\gamma_{esc} \sim 2.5+0.17\ln(R/L)$ and consequently we obtain the anomalous exponent $\mu \sim 0.5 + 0.17\ln(R/L)$ for the sticky region.

The ETs from the long living trajectories present significant characteristics of sticky motion for $R/L = 1/1000, 1/100, 1/10$. In other words, sticky motion and long living trajectories start to occur for *very* small rounding borders: around 0.1% from the whole billiard size is sufficient to generate the sticky motion and change the output signal. Visually such borders are almost negligible. Take for example the border in Fig. 1, it has a ratio $R/L \sim 1/143$.

III. ROUNDING BORDERS GENERATING THE RICH DYNAMICS

The physics involved in the dynamics becomes more evident when the ETs (τ) and escape angles θ_f are plotted as function of the initial incoming angle θ_0 and for different ratios R/L. These plots are shown in Fig. 3 and were generated by using 500×500 points in the intervals $0.01 \leq \theta_0 \leq 1.0$ and $0.00355 \leq R/L \leq 1.0$ $[-8.0 \leq \log(R/L) \leq 0.0]$. We start discussing Fig. 3(a), where each color represents a given value of the ETs written as $\log(\tau)$ (See the colobar on the right). Horizontal stripes with different colors are evident for a significant range of R/L values. Each stripe is defined by a bunch of initial conditions which leave to the same ET and consequently have the same color. For example, for some specific initial angles ($\theta_0 \sim 0.39, 0.56, 0.69, 0.89$) we observe dark blue stripes which correspond to very short ETs. For $R/L = 0$ these angles can be obtained analytically for periodic orbits (for the close billiard) with period $2n$. They are $\theta_0^{(n)} = \arctan\left[\frac{D}{2nL}\right]$, where $n = 1, 2, 3, \ldots$, which is the middle value of the main dark blue stripes which are born at $R/L = 0$. The corresponding ETs are $t_n = nt$, where t is ETs from the case $n = 1$, explained below. The shortest ET ($t_0 \sim 8, 0$) occurs for $\theta_0 \sim 0.0$, where the particle collides once against the wall in front of the escape hole and than leaves the billiard [see trajectory A_1 in Fig. 1]. The width of the stripes are always related to the aperture a from the hole. The next shortest ETs ($t_1 = t \sim 12.8$) occurs for $n = 1$ at $\theta^{(1)} = \arctan 5.0/4.0 \sim 0.89$ where the particle collides directly with the edge of the billiard. See trajectory A_2 in Fig. 1. The third shortest ETs ($\sim 2t$) occurs for $\theta^{(2)} = \arctan 5.0/8.0 \sim 0.56$ and is shown by trajectory A_4 in Fig. 1. We classify these trajectories as A_{2n} and, as we will see later, are the starting point from the Arnold tongues. In the limit $\theta_0 \to \pi/2$ the ETs tend to increase since the trajectories are parallel to the escape point. The ETs statistics for these trajectories will not be considered here, since the large ET is artificially created due to the location of the escape point in the horizontal axis. As n increases the ETs from the trajectories A_{2n} increase, the corresponding stripes assume other colors (light blue $\to$ green $\to$ yellow) [see Fig. 3(a)] and their widths decrease. This is the main behavior of the ETs and stripes close to $R/L \sim 0.0$.

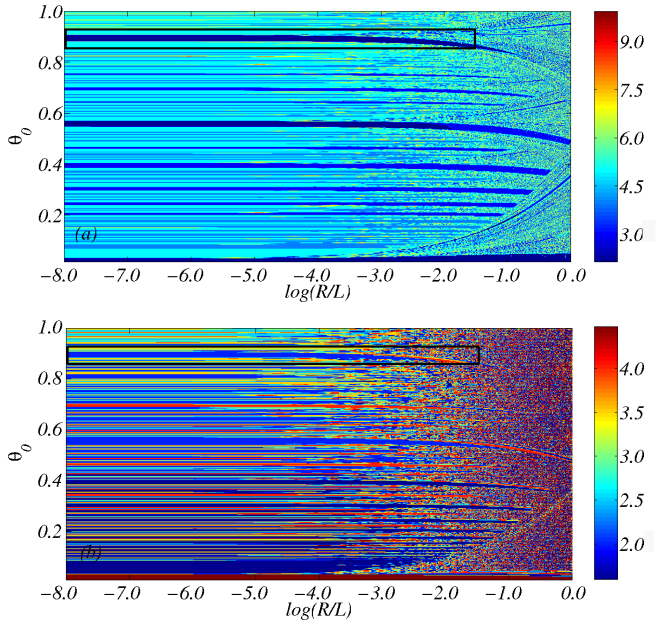

FIG. 3. (Color online) (a) Log of the escape time and (b) emission angle θ_f as a function of $\log(R/L)$ and θ_0.

Increasing R/L we observe in Fig. 3(a) that the stripes for shorter ETs (dark blue) tend to survive longer the bounding border effect, while the stripes for larger ETs (light blue, green and yellow) tend to be destroyed, or even to mix themselves. Notation: we call the dark blue stripes as the *main stripes* and the other stripes as the *secondary stripes*. Therefore, secondary stripes are always related to intermediate and larger values of ETs. Arnold tongues [34] are visible in Fig. 3(a) for $\log(R/L) \gtrsim -4.0$ and are born around the main stripes with frequencies $1/1, 1/2, 1/4, \ldots$. Their relation with the trajectories from Fig. 1 is: $A_1 \to 1/1$, $A_2 \to 1/2$, $A_4 \to 1/4, \ldots$. Outside the main stripes the dynamics becomes very rich and complex. Before explaining how this occurs, we would like to bring to attention the rich dynamics generated by the rounding effects.

Figure 3(b) shows θ_f as a function of $\log(R/L)$ and θ_0. Each color is now related to one emission angle θ_f (see the colorbar). These emission angles vary between $\theta_f \sim 1.4$ (almost horizontally to the left) and $\theta_f \sim 4.5$ (almost horizontally to the right). As in Fig. 3(a), also

here stripes with different colors are evident for a significant range of R/L values. Each stripe is defined by a bunch of initial conditions which leave to the same θ_f. In most cases these stripes occur for the same values of θ_0 from Fig. 3(a). However, two stripes with the same color (same ETs) in Fig. 3(a) have not necessarily the same color (same θ_f) in Fig. 3(b). In other words, different escape angles can have the same ETs. As R/L increases more and more, some stripes survive while the other ones are destroyed or mixed, as in Fig.3(a). The emission angles show a very rich dynamics due to the increasing rounded borders, alternating between all possible colors. This will be discussed below in more details.

IV. ROUNDING BORDERS GENERATING BACKGAMMON STRIPES

In Fig. 4(a) and (b) we show, respectively, a magnification for $\log(\tau)$ and θ_f close to the first region. The magnification is taken around the trajectory A_2 (see Fig. 1) which has a short ETs (main stripe). We observe in Fig. 4(a) that above the main stripe the ETs dynamics changes significantly when R/L increases: larger (light blue and yellow) and shorter (dark blue) ETs appear inside a secondary stripe. This secondary stripe increases linearly its width with R/L. For the emission angle [see Fig. 4(b)] we see a very rich dynamics emerging inside such a secondary stripe, alternating between all possible colors (all emission angles). In addition, below the main stripe a sequence of secondary stripes appear in the light blue background, as can observed in the magnification shown in Fig. 5(a). The width of each stripe in this sequence increases with R/L, remembering stripes from a backgammon board. Notation: secondary stripes with increasing width will be referred as "backgammon stripes". Stickiness and the power law behavior observed in Fig. 2 are born for initial angles which start inside the backgammon stripes. These are the initial conditions which collide, at least once, with the rounded border. The emergence of the power law behavior becomes more evident if we compare Fig. 5(a) with the emission angle behavior shown in Fig. 5(b). The light blue background observed in Fig. 5(a), which corresponds to *one* ETs, has two colors (blue and orange) in Fig. 5(b), which correspond to *two* emission angles (~ 2.1 and ~ 3.5). Interesting is that the sequence of backgammon stripes in Fig. 5(a), and the corresponding multicolor backgammon stripes from Fig. 5(b), are born exactly at the boundary between the blue and orange escape angles at $R/L \sim 0$. Inside the backgammon stripes the range of allowed ETs increases very much. This can be observed by noting the increasing number of yellow and red points. The dynamics involved in the emission angles inside the backgammon stripes is also impressive, showing that tiny changes or errors in the initial angle may drastically change the emission angle.

The key observation here is that the dynamics *inside* the backgammon stripes is the consequence of trajectories which collide with the *inner part* of the semicircle from the escape point, generating the power law behavior for $Q(\tau)$ (see Fig. 2). Another observation is that the location of the backgammon stripes itself is not self-similar but *inside* the backgammon stripes the self-similar structure is evident. Many simulations (not shown) were performed to check this statement. As R/L increases more and more, the self-similar structures increase very fast, *always* in form of backgammon stripes which emerge at different initial angles at $R/L \sim 0.0$ (this was checked for many other initial angles). A simple geometrical calculation determines the angle interval $[-\theta^*, \theta^*]$ for which at least one collision with the rounded border occurs, where

$$\theta^* = \arctan\left\{\frac{\sin\alpha}{(1-\cos\alpha)+a/2R}\right\},$$

and α is the collision angle of the trajectory with the rounded border, defined relative to the center of the semicircle. The interval $[-\theta^*, \theta^*]$ defines the border lines of the backgammon stripes. The larger ETs which appear inside the backgammon stripes start to dissapear when the chaotic region is reached close to $R/L \sim 1.0$.

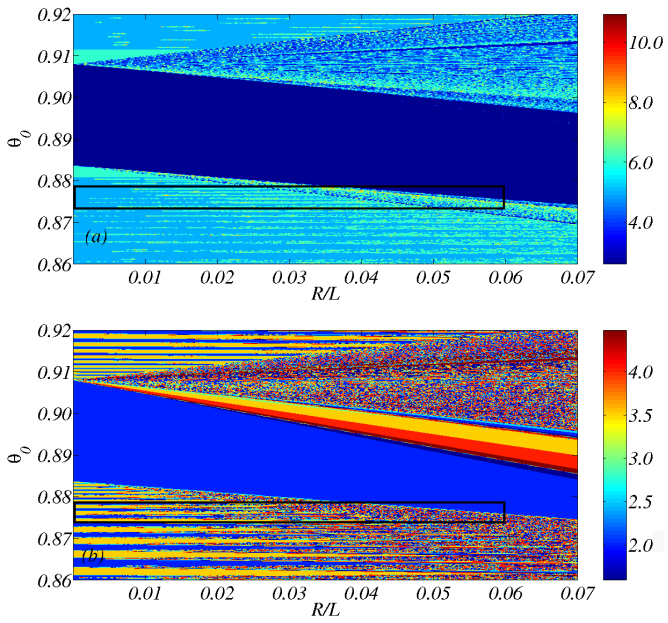

FIG. 4. (Color online) Magnifications from the boxes shown in Fig. 3 (a) and (b), respectively.

V. CONCLUSIONS

Since experiments usually measure a signal coming out from the system of interest, the description of open physical devices is of utmost relevance. For experiments at the frontier of technological limitations, the open set (the

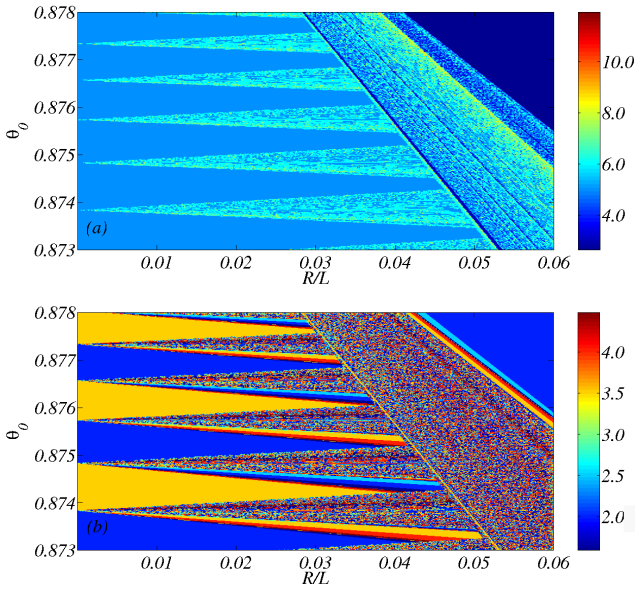

FIG. 5. (Color online) Magnifications from the boxes shown in Fig. 4, respectively.

escape point or hole) can present irregularities or defects which may induce undesirable and intrinsic changes in the outcoming signal. In this work we show that rounded borders in the open set generate a rich dynamics in the integrable rectangular billiard. The escape times statistics for the long-lived trajectories present characteristic of sticky motion when the rounded border represents around $0.1\% \to 10\%$ from the whole billiard size. In this sticky region the escape times decay exponent γ_{esc} increases with R/L and approaches $\gamma_{esc} \sim 2.0$ for $R/L = 1/10$ (R is the radius of the rounded border and L is the height of the billiard). Emission angles and escape times show a self-similar structure only for initial angles inside backgammon like stripes which are born at the integrable case $R/L = 0$. Trajectories which start inside the backgammon stripes will collide, at least once, with the rounded border, generating the power law behavior. As R/L increases more and more, different backgammon stripes start to overlap and the exponent $\gamma_{esc} \sim 2.0$ is obtained. For $R/L = 1.0$ the exponential decay for the escape times is reached, which corresponds to the chaotic motion.

From the nonlinear perspective our results are impressive, showing that a very rich dynamics and stickiness comes alone from tiny border effects ($\sim 0.1\%$) in integrable billiards. Such effects, including the Arnold tongues, should be visible directly in experiments with open integrable devices, open systems with leaks (see [16] and therein cited references) and also in problems related to conduction fluctuations in semiconductors [11, 14], particles transport in nanostructures and cold atoms in open optical billiards [15].

Instead of rounded borders, other shapes for the open sets could be used. All of them should generate sticky motion in integrable billiards, strongly affecting the outcoming signal. Our results will change quantitatively when the aperture a increases, however, in such cases long-lived trajectories will disappear and the statistical analysis for the escape times is not adequate anymore. In this work we considered an integrable billiard as the starting point. We also performed extensive numerical simulations to study rounded border effects in the stadium billiard, which is already chaotic without border effects ($R/L = 0$). For all values of R/L we found that the escape times statistic has an exponential decay, expected for the chaotic behavior.

ACKNOWLEDGMENTS

The authors thank CNPq, CAPES and FINEP (under project CT-INFRA/UFPR) for partial financial support. They also thank E. Altmann and C. Manchein for helpfull discussions.

[1] F. Libisch, C. Stampfer, and J. Burgdörfer, Phys. Rev. B **79**, 115423 (2009).
[2] E. Bogomolny, M. R. Dennis, and D. Dubertrand, J. Phys. A **41**, 335102 (2009).
[3] M. V. Berry and M. R. Dennis, J. Phys. A **41**, 135203 (2008).
[4] H. A. Oliveira, C. Manchein, and M. W. Beims, Phys. Rev. E **78**, 046208 (2008).
[5] M. W. Beims, C. Manchein, and J. M. Rost, Phys. Rev. E **76**, 056203 (2007).
[6] J. Wiersig, Phys. Rev. A **67**, 023807 (2003).
[7] C. Vaa, P. M. Koch, and R. Blümel, Phys. Rev. E **72**, 056211 (2005).
[8] R. Dubertrand, E. Bogomolny, N. Djellali, M. Lebental, and C. Schmit, Phys. Rev. A **77**, 013804 (2008).
[9] H. Bruus and N. D. Whelan, Nonlinearity **9**, 1023 (1996).
[10] D. Alonso and P. Gaspard, J. Phys. A **27**, 1599 (1994).
[11] C. Marlow, R. Taylor, T. Martin, B.C.Scannell, H. Linke, M. Fairbanks, G. Hall, I. Shorubalko, L. T. Fromhold, C. Brown, et al., Phys. Rev. B **73**, 195318 (2006).
[12] A. S. Sachrajda, R. Ketzmerick, C. Gould, Y. Feng, P. J. Kelly, A. Delage, and Z. Wasilewski, Phys. Rev. Lett. **80**, 1948 (1998).
[13] Y. Takagaki, K. H. Ploog, L.-H. Lin, N. Aoki, and Y. Ochiai, Phys. Rev. B **62**, 10255 (2000).
[14] H. Hennig, R. Fleischmann, L. Hufnagel, and T. Geisel, Phys. Rev. E **76**, 015202 (2007).
[15] A. Kaplan, N. Friedman, M. Andersen, and N. Davidson, Phys. Rev. Lett. **87**, 274101 (2001).
[16] E. G. Altmann and T. Tél, Phys. Rev. E **79**, 016204

(2009).
[17] C. P. Dettmann and O. Georgiou, Physica D **238**, 2395 (2009).
[18] L. A. Bunimovich and C. P. Dettmann, Europhys. **80**, 40001 (2007).
[19] D. N. Armstead, B. R. Hunt, and E. Ott, Physica D **193**, 96 (2004).
[20] G. M. Zaslavski, Phys. Rep. **371**, 461 (2002).
[21] S. Tomsovic and A. Lakshminarayan, Phys. Rev. E **76**, 036207 (2007).
[22] C. Manchein, M. W. Beims, and J. M. Rost, arXiv:0907.4181 (2009).
[23] R. Artuso and C. Manchein, Phys. Rev. E **80**, 036210 (2009).
[24] K. A. Mitchell and B. Ilan, Phys. Rev. A **80**, 043406 (2009).
[25] K. A. Mitchell and D. A. Steck, Phys. Rev. A **76**, 031403 (2007).
[26] P. Hansen, K. A. Mitchell, and J. B. Delos, Phys. Rev. E **73**, 066226 (2006).
[27] R. Ketzmerick, Phys. Rev. B **54**, 10841 (1996).
[28] E. G. Altmann, A. Motter, and H. Kantz, CHAOS **15**, 033105 (2005).
[29] J. D. Meiss, Chaos **7**, 139 (1997).
[30] G. Zumofen and J. Klafter, Phys. Rev. E **59**, 3756 (1999).
[31] Y. G. Sinai, Func. Anal. Appl. **2**, 61 (1968).
[32] L. A. Bunimovich, Math. Phys. **65**, 295 (1979).
[33] P. Gaspard and J. R. Dorfman, Phys. Rev. E **52**, 3525 (1995).
[34] A. J. Lichtenberg and M. A. Lieberman, *Regular and Chaotic Dynamics* (Springer-Verlag, 1992).